Transient dynamics in structures with non-homogeneous uncertainties induced by complex joints

J. Duchereau, Christian Soize

Transient dynamics in structures with non homogeneous uncertainties induced by complex joints

J. Duchereau

Department DDSS, Office National d'Etudes et de Recherches Aérospatiales,

Châtillon-sous-Bagneux, France

C. Soize

Laboratoire de Mécanique, Université de Marne-la-Vallée,

Marne-la-Vallée, France

Full Postal address of the corresponding author :

Prof. C. Soize

Laboratoire de mécanique

Université de Marne-la-Vallée

5, bd Descartes

77454 Marne-la-Vallée Cedex 02

France

ABSTRACT : This paper deals with numerical models for prediction of transient dynamical response induced by shocks upon structures with complex joints and shows experimental comparisons. The usual numerical methods for analyzing such structures in the low- and medium-frequency ranges consist in using reduced matrix models constructed with the elastic modes. The contribution of the higher modes is very sensitive to the model errors and to the data errors. In this paper, a nonparametric probabilistic method is applied to construct the random matrix model allowing model errors and data errors to be taken into account. The paper presents an extension of the nonparametric method for the case of non homogeneous model errors through the structure. A dynamic substructuring method is then used and the nonparametric probabilistic model of random uncertainties is used in each substructure with its own level of uncertainties. This approach is applied to a dynamical system made of two plates attached by a complex joint. Experiments have been performed and are used to validate the probabilistic predictive model.

KEYWORDS : shocks, random uncertainties, structural dynamics, probabilistic method, modeling, simulation, experiments.

1. INTRODUCTION

This paper deals with numerical model for predicting transient dynamical response of structures with random uncertainties, excited by a shock. Shock-induced transient dynamics phenomena are widely investigated in the literature. Two kinds of approaches are generally used: the Finite Elements methods (FEM) (see for instance Refs. [1-4]) or the Statistical Energy Analysis method (see for instance Refs. [5, 6]). The present paper concerns transient phenomena for which elastic modes can be used for describing the transient response in the low- and the medium-frequency ranges. Consequently, the FEM is used. Due to the presence of complex substructures having a high level of model uncertainties, such as a complex joint, a probabilistic approach is favoured.

The FE model of such mechanical systems is uncertain (1) due to model uncertainties (for instance, modeling a complex joint by a simple subsystem) and (2) due to data uncertainties (geometry, boundary conditions, constitutive equations). In order to improve the robustness of the predictions, the model uncertainties and the data uncertainties have to be considered. In structural dynamics, data uncertainties are usually taken into account through parametric models (see for instance Refs. [7, 8]). Recently, a nonparametric probabilistic model of random uncertainties has been introduced [9] in structural dynamics. This nonparametric approach allows model uncertainties and data uncertainties to be taken into account in order to increase the robustness of the predictions. This nonparametric probabilistic approach is constructed by using (1) the mean finite element model and (2) a set of random matrix constructed with the Maximum Entropy Principle [10-12]. The mean model corresponds to the nominal finite element model usually developed for the predictions of the dynamical

responses. The random equations of the stochastic system are solved by numerical method through a Monte-Carlo numerical simulation.

Since the nonparametric probabilistic model is a direct construction of the probability distribution of the random operators of the structure, which can then be defined as a global approach for a structure, for the case of non homogeneous uncertainties, the implementation of the nonparametric probabilistic model needs a dynamic substructuring method (for example, the Craig and Bampton method [13]). In this context, works have been carried out in the field of harmonic responses [14]. Here the nonparametric approach is extended to the prediction of shock-induced transient responses for structures with spatially non homogeneous uncertainties [15]. The probabilistic numerical prediction are compared with experiments [16].

In Section 2, the equations of the mean model by dynamic substructuring are presented, Section 3 summarizes the implementation of the nonparametric probabilistic model allowing model uncertainties to be taken into account for the non homogeneous case. The observations of the dynamical system are carried out by shock response spectra. Section 4 deals with the construction of the confidence regions of the shock response spectra. Section 5 is devoted to experiments whereas Sections 6 and 7 compare the predictions with the experiments.

2. EQUATIONS OF THE MEAN MODEL BY DYNAMIC SUBSTRUCTURING

Let us consider the transient response of a fixed structure with a linear constitutive equation, slightly damped, subjected to a deterministic impulsive external load $f_{ext}(t)$. The dynamic subtructuring method with fixed interface (Craig and Bampton [13]) is used. The extension to

the case of a free structure is straightforward. The structure $\mathbb{S}$ is divided into N_S substructures $\mathbb{S}^r$, where $r = 1,\ldots,N_S$. One or several substructures are fixed on a part of their boundary. Every substructure is connected through a coupling interface Σ^r to one (or more) substructure. The equation of the mean model for substructure $\mathbb{S}^r$ with free coupling interface Σ^r, is

$$\begin{aligned} &\left[\underline{\mathbb{M}}^r\right]\underline{\ddot{\mathbf{u}}}^r(t)+\left[\underline{\mathbb{D}}^r\right]\underline{\dot{\mathbf{u}}}^r(t)+\left[\underline{\mathbb{K}}^r\right]\underline{\mathbf{u}}^r(t)=\underline{\mathbf{f}}^r(t), \qquad t\geq 0 \\ &\underline{\dot{\mathbf{u}}}^r(0)=0, \quad \underline{\mathbf{u}}^r(0)=0, \end{aligned} \tag{1}$$

$\underline{\mathbf{u}}^r(t)$ is the $\mathbb{R}^{n^r}$-valued vector of the n^r degrees of freedom (DOF), $\underline{\mathbf{f}}^r(t)$ is the $\mathbb{R}^{n^r}$-valued vector of the external and coupling forces and where $\left[\underline{\mathbb{M}}^r\right]$, $\left[\underline{\mathbb{D}}^r\right]$ and $\left[\underline{\mathbb{K}}^r\right]$ are the mass, damping and stiffness symmetric matrices. Matrix $\left[\underline{\mathbb{M}}^r\right]$ is positive definite and matrices $\left[\underline{\mathbb{D}}^r\right]$ and $\left[\underline{\mathbb{K}}^r\right]$ are positive definite (e. g. fixed substructure) or positive semidefinite (e. g. free substructure). Vectors $\underline{\mathbf{u}}^r(t)$ and $\underline{\mathbf{f}}^r(t)$ are partitioned into n_i^r internal DOF and $n_\Sigma^r = n^r - n_i^r$ coupling interface DOF

$$\underline{\mathbf{u}}^r(t)=\begin{bmatrix}\underline{\mathbf{u}}_i^r(t)\\ \underline{\mathbf{u}}_\Sigma^r(t)\end{bmatrix}, \qquad \underline{\mathbf{f}}^r(t)=\begin{bmatrix}\underline{\mathbf{f}}_i^r(t)\\ \underline{\mathbf{f}}_j^r(t)+\underline{\mathbf{f}}_\Sigma^r(t)\end{bmatrix}, \tag{2}$$

where $\underline{\mathbf{f}}_\Sigma^r(t)$ is relative to the coupling forces applied to the coupling interface Σ^r, $\underline{\mathbf{f}}_i^r(t)$ and $\underline{\mathbf{f}}_j^r(t)$ are due to the external forces applied to substructure $\mathbb{S}^r$. The equation of motion for the reduced matrix model of substructure $\mathbb{S}^r$ can be written as

$$\left[\underline{M}^r\right]\begin{bmatrix}\underline{\ddot{\mathbf{q}}}^r(t)\\ \underline{\ddot{\mathbf{u}}}_\Sigma^r(t)\end{bmatrix}+\left[\underline{D}^r\right]\begin{bmatrix}\underline{\dot{\mathbf{q}}}^r(t)\\ \underline{\dot{\mathbf{u}}}_\Sigma^r(t)\end{bmatrix}+\left[\underline{K}^r\right]\begin{bmatrix}\underline{\mathbf{q}}^r(t)\\ \underline{\mathbf{u}}_\Sigma^r(t)\end{bmatrix}=\begin{bmatrix}\underline{\mathcal{F}}_{N^r}^r(t)\\ \underline{\mathcal{F}}_\Sigma^r(t)\end{bmatrix}, \tag{3}$$

in which the reduced matrices $\left[\underline{M}^r\right]$, $\left[\underline{D}^r\right]$ and $\left[\underline{K}^r\right]$ are such that

$$
\begin{aligned}
\left[\underline{M}^r\right] &= \left[\underline{H}^r\right]^T \left[\underline{\mathbb{M}}^r\right]\left[\underline{H}^r\right], \\
\left[\underline{D}^r\right] &= \left[\underline{H}^r\right]^T \left[\underline{\mathbb{D}}^r\right]\left[\underline{H}^r\right], \\
\left[\underline{K}^r\right] &= \left[\underline{H}^r\right]^T \left[\underline{\mathbb{K}}^r\right]\left[\underline{H}^r\right].
\end{aligned} \tag{4}
$$

In Equation (3), $\underline{\mathbf{q}}^r(t)$ is the $\mathbb{R}^{N^r}$-valued vector of the generalized DOF relative to the N^r first elastic modes with fixed coupling interface, $\underline{\mathbf{u}}^r_\Sigma(t)$ are the coupling interface DOF and $\left[\underline{H}^r\right]$ is the transformation matrix expressed by means of the $\left(n^r_i \times N^r\right)$ modal matrix $\left[\underline{\Phi}^r\right]$ and of the $\left(n^r_i \times n^r_\Sigma\right)$ matrix $\left[\underline{S}^r_\Sigma\right]$ of the static boundary functions

$$
\begin{bmatrix} \underline{\mathbf{u}}^r_i(t) \\ \underline{\mathbf{u}}^r_\Sigma(t) \end{bmatrix} = \left[\underline{H}^r\right] \begin{bmatrix} \underline{\mathbf{q}}^r(t) \\ \underline{\mathbf{u}}^r_\Sigma(t) \end{bmatrix} \quad \text{and} \quad \left[\underline{H}^r\right] = \begin{bmatrix} \left[\underline{\Phi}^r\right] & \left[\underline{S}^r_\Sigma\right] \\ 0 & \left[I_{n_\Sigma}\right] \end{bmatrix}, \tag{5}
$$

in which $\left[I_{n_\Sigma}\right]$ is the $\left(n^r_\Sigma \times n^r_\Sigma\right)$ unity matrix. In Eq. (3), $\underline{\mathcal{F}}^r_{N^r}(t)$ and $\underline{\mathcal{F}}^r_\Sigma(t)$ are such that $\underline{\mathcal{F}}^r_{N^r}(t) = \left[\underline{\Phi}^r\right]^T \underline{\mathbf{f}}^r_i(t)$ and $\underline{\mathcal{F}}^r_\Sigma(t) = \left[\underline{S}^r_\Sigma\right] \underline{\mathbf{f}}^r_i(t) + \underline{\mathbf{f}}^r_j(t) + \underline{\mathbf{f}}^r_\Sigma(t)$. The reduced matrix models of the substructures are usually assembled using the continuity of displacements and the equilibrium of the interacting forces on the coupling interfaces.

3. NONPARAMETRIC PROBABILISTIC MODEL

The structure exhibits subdomains with various levels of uncertainty (non homogeneous uncertainties). Consequently, the substructuring is fit so that each substructure can be considered as homogeneous with respect to its level of uncertainties. Thus, the uncertainty level differs from one substructure to another one. The nonparametric probabilistic model of uncertainty is implemented independently for each substructure.

3.1 Construction principle of a nonparametric model of random uncertainties for each substructure

The nonparametric probabilistic approach [9] consists in directly constructing the probabilistic model of the generalized random matrices for each substructure. Let $\mathbf{U}^r(t)$ be the random vector of the n^r DOF of substructure $\mathbb{S}^r$ with free coupling interface. Vector $\mathbf{U}^r(t)$ can be written as

$$\mathbf{U}^r(t) = \begin{bmatrix} \mathbf{U}_i^r(t) \\ \mathbf{U}_\Sigma^r(t) \end{bmatrix} = \left[\underline{H}^r\right] \begin{bmatrix} \mathbf{Q}^r(t) \\ \mathbf{U}_\Sigma^r(t) \end{bmatrix}, \tag{6}$$

in which $\mathbf{Q}^r(t)$ is the $\mathbb{R}^{N^r}$-valued random vector of the generalized DOF and $\mathbf{U}_\Sigma^r(t)$ is the $\mathbb{R}^{n_\Sigma^r}$-valued random vector of the coupling interface DOF. The stochastic process $(\mathbf{Q}^r,\ \mathbf{U}_\Sigma^r)$ indexed by $[0,+\infty[$ with values in $\mathbb{R}^{\mu^r}$, with $\mu^r = N^r + n_\Sigma^r$, is such that

$$\left[\mathbf{M}^r\right] \begin{bmatrix} \ddot{\mathbf{Q}}^r(t) \\ \ddot{\mathbf{U}}_\Sigma^r(t) \end{bmatrix} + \left[\mathbf{D}^r\right] \begin{bmatrix} \dot{\mathbf{Q}}^r(t) \\ \dot{\mathbf{U}}_\Sigma^r(t) \end{bmatrix} + \left[\mathbf{K}^r\right] \begin{bmatrix} \mathbf{Q}^r(t) \\ \mathbf{U}_\Sigma^r(t) \end{bmatrix} = \begin{bmatrix} \underline{\boldsymbol{\mathcal{F}}}_{N^r}^r(t) \\ \boldsymbol{\mathcal{F}}_\Sigma^r(t) \end{bmatrix}, \qquad t > 0 \tag{7}$$

in which $\left[\mathbf{M}^r\right]$ is a random matrix with values in the set $\mathbb{M}_{\mu^r}^+(\mathbb{R})$ of all the symmetric positive-definite $\left(\mu^r \times \mu^r\right)$ real matrices and, $\left[\mathbf{D}^r\right]$ and $\left[\mathbf{K}^r\right]$ are random matrices with values in $\mathbb{M}_{\mu^r}^+(\mathbb{R})$ (for a fixed substructure) or in the set $\mathbb{M}_{\mu^r}^{+\,0}(\mathbb{R})$ of all the symmetric positive-semidefinite $\left(\mu^r \times \mu^r\right)$ real matrices (for a free substructure). In Eq. (7), the random vector $\boldsymbol{\mathcal{F}}_\Sigma^r(t)$ is such that $\boldsymbol{\mathcal{F}}_\Sigma^r(t) = \left[\underline{S}_\Sigma^r\right]^T \underline{\mathbf{f}}_i^r(t) + \underline{\mathbf{f}}_j^r(t) + \mathbf{F}_\Sigma^r(t)$, in which $\mathbf{F}_\Sigma^r(t)$ the random vector of the coupling forces at interface Σ^r.

By construction of the nonparametric model, we have

$$E\left\{\left[\mathbf{M}^r\right]\right\} = \left[\underline{M}^r\right], \quad E\left\{\left[\mathbf{D}^r\right]\right\} = \left[\underline{D}^r\right], \quad E\left\{\left[\mathbf{K}^r\right]\right\} = \left[\underline{K}^r\right], \tag{8}$$

where E is the mathematical expectation. In the next section, we give a short description of the probabilistic model for random matrices $[\mathbf{M}^r]$, $[\mathbf{D}^r]$ and $[\mathbf{K}^r]$.

3.2 Probabilistic model for the random matrices

Below, the random matrix $[\mathbf{A}^r]$ denotes random matrices $[\mathbf{M}^r]$, $[\mathbf{D}^r]$ or $[\mathbf{K}^r]$. The mean value of random matrix $[\mathbf{A}^r]$ is denoted by $[\underline{A}^r]$ and consequently, $[\underline{A}^r] = E\{[\mathbf{A}^r]\}$ denotes deterministic matrices $[\underline{M}^r]$, $[\underline{D}^r]$ or $[\underline{K}^r]$ (see Eq. (8)).

When real matrix $[\underline{A}^r]$ is positive definite, then an upper triangular $(\mu^r \times \mu^r)$ real matrix $[\underline{L}_{A^r}]$ exists such that $[\underline{A}^r] = [\underline{L}_{A^r}]^T [\underline{L}_{A^r}]$ (Cholesky factorization). In this case, we let $m^r = \mu^r$. When matrix $[\underline{A}^r]$ is with a rank equal to $\widetilde{m}^r < \mu^r$, then a $\widetilde{m}^r \times \mu^r$ real matrix $[\underline{L}_{A^r}]$ exists such that $[\underline{A}^r] = [\underline{L}_{A^r}]^T [\underline{L}_{A^r}]$. For instance, this matrix $[\underline{L}_{A^r}]$ can be obtained from the eigenvectors related to the non-zero eigenvalues of matrix $[\underline{A}^r]$, but other constructions exist. In this case, we let $m^r = \widetilde{m}^r$. For both cases, random matrix $[\mathbf{A}^r]$ can then be written as $[\mathbf{A}^r] = [\underline{L}_{A^r}]^T [\mathbf{G}_{A^r}] [\underline{L}_{A^r}]$ in which $[\mathbf{G}_{A^r}]$ is an $\mathbb{M}^+_{m^r}(\mathbb{R})$-valued random matrix whose probability distribution is defined below. The probability distribution $P_{[\mathbf{G}_{A^r}]}$ of random matrix $[\mathbf{G}_{A^r}]$ is constructed by using the maximum entropy principle [9] and is defined by a probability density function $[G] \mapsto p_{[\mathbf{G}_{A^r}]}([G])$ from $\mathbb{M}^+_{m^r}(\mathbb{R})$ into $\mathbb{R}^+ = [0, +\infty[$, with respect to the measure (volume element) $\tilde{d}G$ on the set $\mathbb{M}^S_{m^r}(\mathbb{R})$ of all the $(m^r \times m^r)$ real symmetric matrices and defined by

$$\tilde{d}G = 2^{m^r\left(m^r-1\right)/4} \prod_{1\leq i\leq j\leq m^r} d[G]_{ij} \, .$$

We then have $P_{\left[\mathbf{G}_{A^r}\right]} = p_{\left[\mathbf{G}_{A^r}\right]}\left([G]\right) \tilde{d}G$, with the normalization condition

$$\int_{\mathbb{M}^+_{m^r}(\mathbb{R})} p_{\left[\mathbf{G}_{A^r}\right]}\left([G]\right) \tilde{d}G \; = \; 1 \, .$$

Probability density function $p_{\left[\mathbf{G}_{A^r}\right]}\left([G]\right)$ is then written as

$$p_{\left[\mathbf{G}_{A^r}\right]}\left([G]\right) = \mathbf{1}_{\mathbb{M}^+_{m^r}(\mathbb{R})}\left([G]\right) \times C_{\mathbf{G}_{A^r}} \times \left(det[G]\right)^{\frac{\left(m^r+1\right)\left(1-\delta^2_{A^r}\right)}{2\delta^2_{A^r}}} \times exp\left\{-\frac{\left(m^r+1\right)}{2\delta^2_{A^r}} tr[G]\right\} \quad (9)$$

in which *det* is the determinant of the matrices,

$\mathbf{1}_{\mathbb{M}^+_{m^r}(\mathbb{R})}\left([G]\right)$ is equal to 1 if $[G] \in \mathbb{M}^+_{m^r}(\mathbb{R})$ and is equal to zero if $[G] \notin \mathbb{M}^+_{m^r}(\mathbb{R})$,

$C_{\mathbf{G}_{A^r}}$ is a positive constant such that

$$C_{\mathbf{G}_{A^r}} = \frac{\left(2\pi\right)^{-m^r\left(m^r-1\right)/4} \left(\frac{m^r+1}{2\delta^2_{A^r}}\right)^{\frac{m^r\left(m^r+1\right)}{2\delta^2_{A^r}}}}{\left\{\prod_{j=1}^{m^r} \Gamma\left(\frac{m^r+1}{2\delta^2_{A^r}} + \frac{1-j}{2}\right)\right\}}$$

where $\Gamma(z)$ is the gamma function defined for $z>0$ by $\Gamma(z) = \int_0^{+\infty} t^{z-1} e^{-t} \, dt$.

The probability distribution of random matrix $\left[\mathbf{G}_{A^r}\right]$ depends only on real parameter δ_{A^r} which is independent of dimension m^r and of frequency ω, and which allows the dispersion of random matrix $\left[\mathbf{A}^r\right]$ to be controlled. This parameter is defined by

$$\delta_{A^r} = \left\{ \frac{E\left\{ \left\| \left[\mathbf{G}_{A^r}\right] - \left[\underline{G}_{A^r}\right] \right\|_F^2 \right\}}{\left\| \left[\underline{G}_{A^r}\right] \right\|_F^2} \right\}. \tag{10}$$

The parameter has to be chosen such that

$$0 < \delta_{A^r} < \sqrt{\frac{m^r + 1}{m^r + 5}}, \tag{11}$$

in which $\left[\underline{G}_{A^r}\right] = E\left\{\left[\mathbf{G}_{A^r}\right]\right\} = \left[I_{m^r}\right]$ and where $\left\|[B]\right\|_F^2 = tr\left([B][B]^T\right)$. The dispersion parameters of random matrices $\left[\mathbf{M}^r\right]$, $\left[\mathbf{D}^r\right]$ and $\left[\mathbf{K}^r\right]$ are then controlled by the parameters δ_{M^r}, δ_{D^r} and δ_{K^r} which are independent of m^r and chosen according to Eq. (11).

The probabilistic model of the entire structure is obtained by the assemblage of the stochastic substructures and the random unknown vector is $\mathbf{U}_e(t) = \left(\mathbf{Q}^1(t), \cdots, \mathbf{Q}^{N_S}(t), \mathbf{U}_\Sigma(t)\right)$, in which $\mathbf{U}_\Sigma(t)$ is the union of the coupling interface DOF $\mathbf{U}_\Sigma^r(t)$.

3.3 Algebraic representation of random matrix $\left[\mathbf{G}_{A^r}\right]$

In order to perform a Monte-Carlo numerical simulation, the following algebraic representation of positive-definite real random matrix $\left[\mathbf{G}_{A^r}\right]$ is given. The random matrix $\left[\mathbf{G}_{A^r}\right]$ with values in $\mathbb{M}_{m^r}^+(\mathbb{R})$, is written

$$\left[\mathbf{G}_{A^r}\right] = \left[\mathbf{L}_G\right]^T \left[\mathbf{L}_G\right], \tag{12}$$

in which $\left[\mathbf{L}_G\right]$ is an upper triangular matrix in $\mathbb{M}_{m^r}(\mathbb{R})$ such that :

(1) the random variables $\left\{ \left[\mathbf{L}_G\right]_{ll'},\ l \leq l' \right\}$ are mutually independent;

(2) for $l < l'$, the real random variable $\left[\mathbf{L}_G\right]_{ll'}$ is such that

$$\left[\mathbf{L}_G\right]_{ll'} = \sigma\, U_{ll'} \qquad \text{with} \qquad \sigma = \frac{\delta_{A^r}}{\sqrt{m^r + 1}}\ , \tag{13}$$

where $U_{ll'}$ is a real-valued Gaussian random variable with zero mean and variance equal to 1;

(3) for $l = l'$, the random variable $\left[\mathbf{L}_G\right]_{ll}$ with values in $\mathbb{R}^+$ is written as

$$\left[\mathbf{L}_G\right]_{ll} = \sigma \sqrt{2\, V_l}\ , \tag{14}$$

with σ defined by Eq. (13) and with V_l a positive-valued gamma random variable whose probability density function $p_{V_l}(v)$ with respect to dv is such that

$$p_{V_l}(v) = \mathbf{1}_{\mathbb{R}^+}(v)\ \left\{\Gamma\left(v_l\right)\right\}^{-1}\ v^{v_l - 1}\ e^{-v} \qquad \text{with} \qquad v_l = \frac{m^r + 1}{2\delta_{A^r}^2} + \frac{1 - l}{2}\ . \tag{15}$$

4 RANDOM SHOCK RESPONSE SPECTRA

The analysis of the numerical model developed and its comparisons with the experiments are carried out by means of Shock Response Spectra (SRS) [17] calculated for the acceleration responses and denoted by $S_a(\xi, \omega)$ in which ξ and ω are the damping ratio and the natural frequency of a single-DOF oscillator used to generate the SRS. The SRS allows a transient response to be described as a function of frequency (see Figure 1).

In presence of uncertainties, the transient response is a time stochastic process and consequently, for fixed ξ, every SRS is a stochastic process indexed by frequency. The stochastic solution of such a problem can be formally written, but the solution involves high-

dimensional multiple integrals which can only be computed by the Monte-Carlo numerical method. Then a direct Monte-Carlo numerical simulation of stochastic Eq. (7) is performed. Each realization of the random matrices is constructed according to the probabilistic model described in Section 3 and using the algorithm presented in Section 3.3. The transient responses for every realization are carried out using the Newmark method (unconditionally stable step-by-step numerical integration scheme [18]). The probabilistic magnitudes describing the random SRS are estimated by the usual mathematical statistics allowing a confidence region to be constructed.

4.1 Confidence region for the random responses

Every random SRS is calculated for a damping ratio $\xi = 0.001$. Each realization of random SRS is computed by using the Newmark integration scheme of the equation of motion. The SRS scale is normalized with respect to $g = 9.81\ m.s^{-2}$. Then, we introduce the normalized random shock response spectra $s(\omega) = S_a(\xi, \omega)/g$. The confidence region of random process $\left\{ s(\omega),\ \omega \in (\omega_1, \omega_2) \right\}$ associated with a given probability level $Pc = 0.95$, is defined by an upper envelope $S^+(\omega)$ and a lower envelope $S^-(\omega)$ such that

$$Prob.\left\{ S^-(\omega) < 10\ log_{10}\left(s(\omega) \right) < S^+(\omega) \right\} \geq Pc\,,$$

$$S^+(\omega) = 10\ log_{10}\left(m_1(\omega) + \frac{\sigma(\omega)}{\sqrt{1-Pc}} \right),$$

$$S^-(\omega) = 2S^0(\omega) - S^+(\omega),$$

with $S^0(\omega) = 10\ log_{10}\left(m_1(\omega) \right)$ which is related to the mean value of the stochastic response and with the first and second order moments $m_1(\omega) = E\left\{ s(\omega) \right\}$,

$m_2(\omega) = E\{s^2(\omega)\}$ and $\sigma(\omega) = \sqrt{m_2(\omega) - m_1^2(\omega)}$ estimated by the usual mathematical statistics.

5. EXPERIMENTS

Experiments are used for validating the proposed nonparametric approach of random uncertainties for transient dynamics induced by shocks in a structure having a complex joint. Experimental results are made up of 21 experiments carried out for the same test specimen.

5.1 Experimental model description

The test specimen [16] consists of two 3mm-thick aluminium (Dural) plates connected together through a complex joint and excited by a deterministic impulsive load. Plate 1 is 0.4m width and 0.6m length. Plate 2 is 0.5m width and 0.6m length. The complex joint is constituted of 2 smaller plates (2mm-thick, 0.14m width, 0.6m length), tightened by 2 lines of 20 bolts (see Figure 2).

The experimental database is constituted of the accelerograms measured with 29 accelerometers for 21 experimental configurations corresponding to 21 random distributions of bolt-prestresses having the same mean values [16]. The experimental set-up corresponds to a free-free structure.

The impulsive loads used in the experiments are deterministic. The two loads that we have chosen to display here range in the medium-frequency band: [1000-1200] Hz (see Figure 3) and [1800-2000] Hz (see Figure 4). The experimental loads for 200 Hz bandwidth are

digitally generated and consequently, the 21 configurations are excited with the same deterministic impulsive load.

5.2 Analysis of experimental results

For each configuration and for the driven force (impulsive load applied to the excitation point), the experimental database is constituted of the normal accelerations measured by 29 accelerometers located to the nodes of a regular grid constituted of 29 points which coincide with nodes of the mean finite element model. In order to limit the number of figures presented in this paper, the experimental results and the comparisons of the experiments with the predictions are limited (for a given impulsive load applied to the excitation point 1 in plate 2, see Fig. 2) to 3 observation points (3 accelerometers). The first one is the driven point (point 1 in plate 2), the second one is an observation point located in the plate where is located the driven point (point 3 in plate 2) and the third point is located in the other plate, through the complex joint (point 2 in plate 1). Additional results and comparisons can be found in Ref. [15].

The experimental results are expressed in terms of SRS and displayed for two observation points (Fig. 2): point 2 is situated on plate 1, whereas point 3 is in plate 2 which is the excited one. In Figure 5 and Figure 6, the pencil of solid lines represents the SRS for 21 experimental configurations at observation points 2 and 3 (see Fig. 2). Figure 5 corresponds to an excitation in band [1000-1200] Hz and Figure 6 corresponds to an excitation in band [1800-2000] Hz. For both bands, the influence of the bolt-prestresses upon the experimental responses is noticeable and increases with the frequency; This emphasizes the sensitivity of higher elastic modes to uncertain parameters of such a system. Moreover, the peaks of the SRS are

smoother as frequency grows. Nevertheless, the dispersion of the experimental responses is more significant for band [1800-2000] Hz than for band [1000-1200] Hz.

6. COMPARISON OF THE EXPERIMENTS WITH THE MEAN MODEL PREDICTION

A FE model is developed for the mean model of this test specimen and allows the response of the mean model to be calculated. Further, the nonparametric probabilistic approach of random uncertainties due to the complex junction is constructed from the mean FE model.

6.1 Mean model

6.1.1 Finite Element model of the mean system

The three substructures of the mean model are represented by a uniform FE model of 4 nodes plates elements following the Kirchhoff thin plate assumptions (e.g. DOF Tz, Rx and Ry are retained). The complete structure is constituted of the 3 substructures (Figure 2): there are 6222 DOF (34x61 nodes) in *plate 1*, 2745 DOF (15x61 nodes) in the *Complex Joint* (CJ) and 8052 DOF (44x61nodes) in *plate 2*, e.g. a total amount of more than 16000 DOF. Plates 1 and 2 are isotropic whereas the complex joint needs an orthotropic description. The updating of the first 3 elastic modes of the complete structure and the associated damping ratios of the mean FE model has been performed using experiments. It should be noted that the responses measured at the 29 accelerometers are sufficient for identifying the first 3 elastic modes which are global bending modes of the complete structure. The mean FE model has to be able to give a reasonable prediction of the mean dynamical response of the mechanical system in the frequency band analysis [0 , 2000] Hz. in order to successfully apply the nonparametric

probabilistic approach. For the numerical mean FE model, there are 64 elastic modes below 1000 Hz, 77 below 1200 Hz, 113 elastic modes below 1800 Hz and 127 elastic modes below 2000 Hz. It should be noted that the mesh of the complete structure constituted of (61x91) nodes is adapted to the frequency band [0 , 2000] Hz. The spatial sampling is the same for the two spatial directions and corresponds to 6 points for the smallest half wave length appearing in the elastic mode having the highest eigenfrequency (close to 2000 Hz) .

6.1.2 Damping model of the mean system

For each substructure $\mathbb{S}^r$, the damping matrix of the mean FE model has then been chosen [19] such that

$$\left[\underline{\mathbb{D}}^r\right] = \sum_{\gamma=1}^{N} 2\,\xi_\gamma \,\frac{\omega_\gamma}{\mu_\gamma}\left[\underline{\mathbb{M}}^r\right]\,\underline{\mathbf{V}}_\gamma^r\;\underline{\mathbf{V}}_\gamma^{rT}\;\left[\underline{\mathbb{M}}^r\right]$$

in which N is such that $1 \leq N \leq n^r$ and where $\underline{\mathbf{V}}_\gamma^r = \begin{bmatrix} \underline{\mathbf{V}}_{\gamma i}^r \\ \underline{\mathbf{V}}_{\gamma \Sigma}^r \end{bmatrix}$, ω_γ and ξ_γ are respectively the eigenmode, the eigenfrequency and the modal damping rate relative to the γ^{th} free interface mode. This mean damping model allows the mean damping matrix of each substructure to be easily constructed, for which the data corresponds to the modal damping rates of the substructure. Taking the same value $\underline{\xi}$ for the modal damping rates ξ_γ of all the elastic modes and for all the substructures, it can easily be verified that the modal damping rates of the complete structure are the same and equal to $\underline{\xi}$ which is then called the "mean damping rate". We have then chosen $N = N^r + n_\Sigma$, $\xi_\gamma = \underline{\xi}$, $\mu_\gamma = 1$ and we directly construct the reduced damping matrix such that

$$\left[\underline{D}^{r}\right] = \sum_{\gamma=1}^{N} 2\ \underline{\xi}\ \omega_{\gamma}\ \underline{\mathbf{C}}_{\gamma}\ \underline{\mathbf{C}}_{\gamma}^{T}$$

with $\underline{\mathbf{C}}_{\gamma} = \left[\underline{H}^{r}\right]^{T}\left[\underline{\mathbb{M}}^{r}\right]\underline{\mathbf{V}}_{\gamma}^{r}$. The value of this mean damping rate $\underline{\xi}$ has been estimated from the measurements related to the modal damping rates of the first 12 elastic modes of the complete structure and yields $\underline{\xi} = 0.0021$. Clearly there is an uncertainty with such a damping model of the substructures, the level of model uncertainties being very important for the complex joint and very small for plates 1 and 2 (see Section 7).

6.2 Mean model results

In Figures 5 ([1000-1200] Hz) and 6 ([1800-2000] Hz), the thick dashed lines denote the responses of the mean model at observation points 2 and 3 (see Fig. 2). For band [1000-1200] Hz, the mean reduced model has 125 = (50 + 8 + 67) elastic modes for the 3 substructures with fixed coupling interfaces and, for band [1800-2000] Hz, the mean reduced model has 205 = (80 + 20 + 105) elastic modes for the three substrucres with fixed coupling interfaces. The mean model prediction's SRS do not agree with the experimental SRS. These significant errors between the experimental and the mean numerical responses cannot be due to the bolt-prestresses. On the contrary, they point out that the model uncertainties in the mean model are important and require model (and data) uncertainties to be taken into account through the proposed nonparametric probabilistic approach.

7. RESULTS OF THE PROBABILISTIC MODEL

A confidence region of the stochastic response of the model with random uncertainties can then be used to predict the responses of the uncertain system and can be compared with the experiment.

In order to evaluate the role played by the nonhomogeneity of uncertainties which are assumed to be larger in the complex joint, a sensitivity analysis with respect to parameters δ^r has been carried out. Below, we limit the presentation to a sampling of the values used. The results are displayed for the following values of the dispersion parameters:

$\delta_M^{CJ} = 0$, $\delta_D^{CJ} = 0.8$ and $\delta_K^{CJ} = 0.7$,

$\delta_M^{plates} = 0$, $\delta_D^{plates} = 0$ and $\delta_K^{plates} = 0.1$,

for both excitation bands: [1000-1200] Hz and [1800-2000] Hz.

The mass of the mean model has been updated with experiments and consequently, there is a negligible error on the mass matrices. The Monte-Carlo numerical simulation method has been carried out for a sufficiently high amount of realizations (600 to 1200), depending on the uncertainty level assigned. A convergence analysis with respect to the number of elastic modes ν in the reduced matrix models has been performed as well. As a consequence, the results are displayed for the 2 following cases:

$\nu = N^1 + N^2 + N^3 = 150$ for [1000-1200] Hz,

$\nu = N^1 + N^2 + N^3 = 232$ for [1800-2000] Hz.

Figures 5 and 6 show the results obtained for these values. The grey region is the 95% confidence region of the random responses, computed with the nonparametric model of random uncertainties. It should be noted that the nonparametric probabilistic model of random

uncertainties allows the 95% confidence region (grey region) to include the experiments although the response of the mean model (dashed lines) does not well fit the experiments (pencil of solid lines).

The nonparametric probabilistic approach of random uncertainties improve significantly the mean model predictions. The confidence regions grow wider as frequency goes up for fixed dispersion parameters δ^r. This outlines the sensitivity of high rank elastic modes to model uncertainties (and data uncertainties).

8. CONCLUSIONS

About uncertainty modeling, the comparisons of the developed model with the experiments show the capability of the nonparametric probabilistic approach to predict the shock-induced transient response in the low- and the medium-frequency ranges. In spite of a rather large number of DOF used in the mean FE model, significant errors appear between experiments and numerical prediction. These errors are mainly due to the simplified model used for modeling the complex junction. It implies that some model uncertainties exist in the mean FE model. The nonparametric approach of non homogeneous uncertainties proposed in this paper allows the robustness of the numerical prediction to be increased. The comparison of the experiments with the confidence region predicted by this probabilistic approach is satisfying for a low- and a medium-frequency band. A general methodology to estimate the values of the dispersion parameters is in progress. The value of the dispersion parameter δ_K^{CJ} is expected to be almost constant whatever the excitation band. For the range of frequency presented here (e. g. medium-frequency bands), the dispersion parameters δ_K^{plates} are small but not negligible.

ACKNOWLEDGEMENTS

The authors thank ONERA which has supported this research.

REFERENCES

1. P. K. Roy and N. Ganesan 1995 *Journal of Sound and Vibration* **183** (5), 873-890. Transient response of a cantilever beam subjected to an impulse load.

2. B. Gangadhara Prusty and S. K. Satsangi 2001 *Journal of Sound and Vibration* **248** (2), 215-233. Finite element transient dynamic analysis of laminated stiffened shells.

3. Y. W. Kim and Y.-S. Lee 2002 *Journal of Sound and Vibration* **252** (1), 1-17. Transient analysis of ring-stiffened composite cylindrical shells with both edges clamped.

4. O. C. C. Zienkiewicz and R. L. Taylor 2000 *Finite Element Method, vol. 1-2-3*. Butterworth-Heinemann.

5. R. H. Lyon and R. G. Dejong 1995 *Theory and Application of Statistical Energy Analysis*. Boston: Butterworth-Heinemann.

6. E. Dalton 1995 *AIAA Journal* , 759-767. Analysis and validation testing of impulsive load response in complex, multi-compartimented structures.

7. E. J. Haug, K. K. Choi, V. Komkov 1986 *Design Sensitivity Analysis of Structural Systems*. San Diego: Academic Press.

8. R. Ghanem and P. D. Spanos 1991 *Stochastic Finite Elements: A Spectral Approach*. New-York: Springer.

9. C. Soize 2001 *Journal of the Acoustical Society of America* **109** (5), 1979-1996. Maximum entropy approach for modeling random uncertainties in transient elastodynamics.

10. C. E. Shannon 1948 *Bell System Technology Journal* **27**, 379-423 and 623-659. A mathematical theory of communication.

11. E. T. Jaynes 1957 *Physical Review* **106** (4), 620-630. Information theory and statistical mechanics.

12. E. T. Jaynes 1957 *Physical Review* **108** (2), 171-190. Information theory and statistical mechanics.

13. R.R. Craig and M.M.C. Bampton 1968 *AIAA Journal* **6**, 1313-1319. Coupling of substructures for dynamic analysis.

14. C. Soize, H. Chebli 2003 *Journal of Engineering Mechanics, ASCE* **129** (4), 449-457. Random uncertainties model in dynamic substructuring using a nonparametric probabilistic model.

15. J. Duchereau 2004 *Modélisation non paramétrique des incertitudes en dynamique transitoire des systèmes complexes avec incertitudes non homogènes*. Thèse de doctorat du Conservatoire National des Arts et Métiers, Paris.

16. M. Menelle, P. Baroin 2001 ONERA 1/05822 DDSS Dynamique transitoire des structures, partie expérimentale.

17. R. W. Clough and J. Penzien 1975 *Dynamics of Structures*. New-York: Mc Graw-Hill.

18. K. J. Bathe and E. L. Wilson 1976 *Numerical Methods in Finite Element Analysis*. New-York: Prentice-Hall.

19. R. Ohayon and C. Soize 1998 *Structural Acoustics and Vibrations*. New York: Academic Press.

FIGURE 1

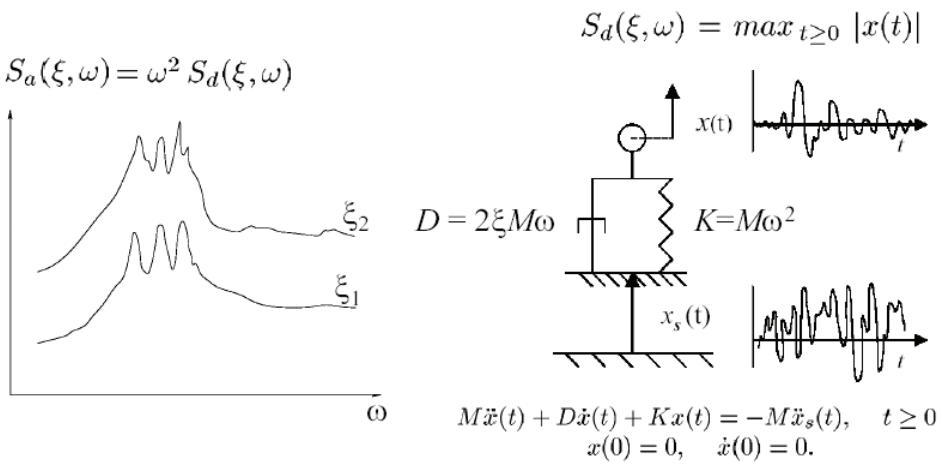
$S_d(\xi,\omega) = max_{t\geq 0} |x(t)|$
$S_a(\xi,\omega) = \omega^2 S_d(\xi,\omega)$
ξ_2
ξ_1
ω
$D = 2\xi M\omega$
$K = M\omega^2$
$x(t)$
$x_s(t)$
t
$M\ddot{x}(t) + D\dot{x}(t) + Kx(t) = -M\ddot{x}_s(t), \quad t \geq 0$
$x(0) = 0, \quad \dot{x}(0) = 0.$

FIGURE 2

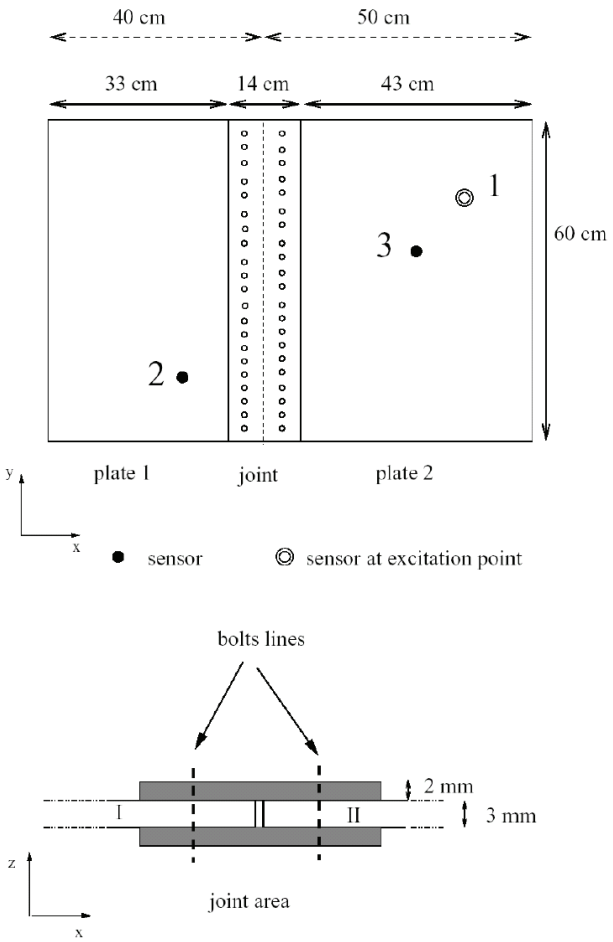
40 cm
50 cm
33 cm
14 cm
43 cm
1
2
3
60 cm
plate 1
joint
plate 2
y
x
sensor
sensor at excitation point
bolts lines
2 mm
3 mm
I
II
z
x
joint area

FIGURE 3

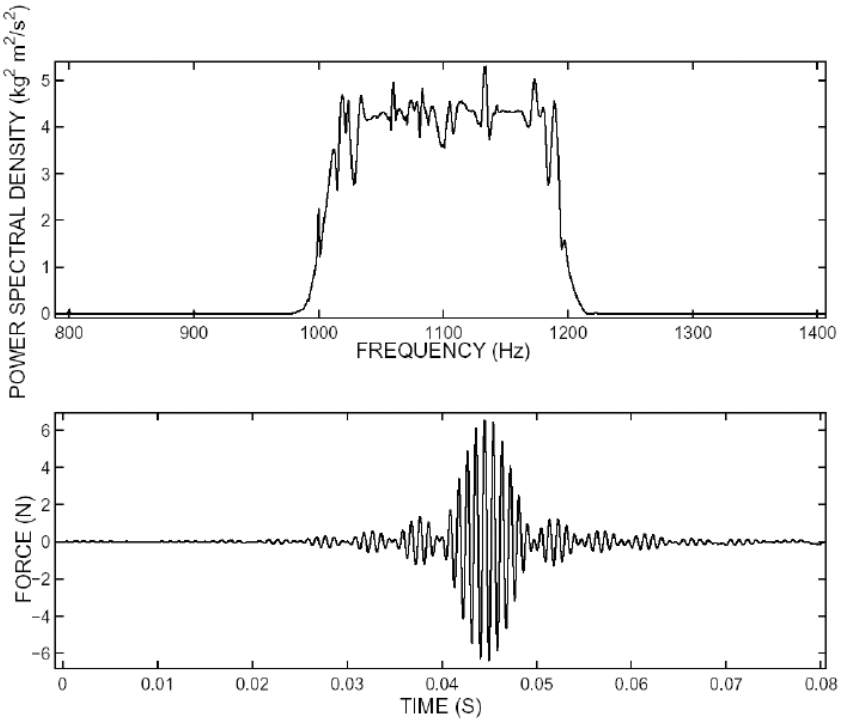

FIGURE 4

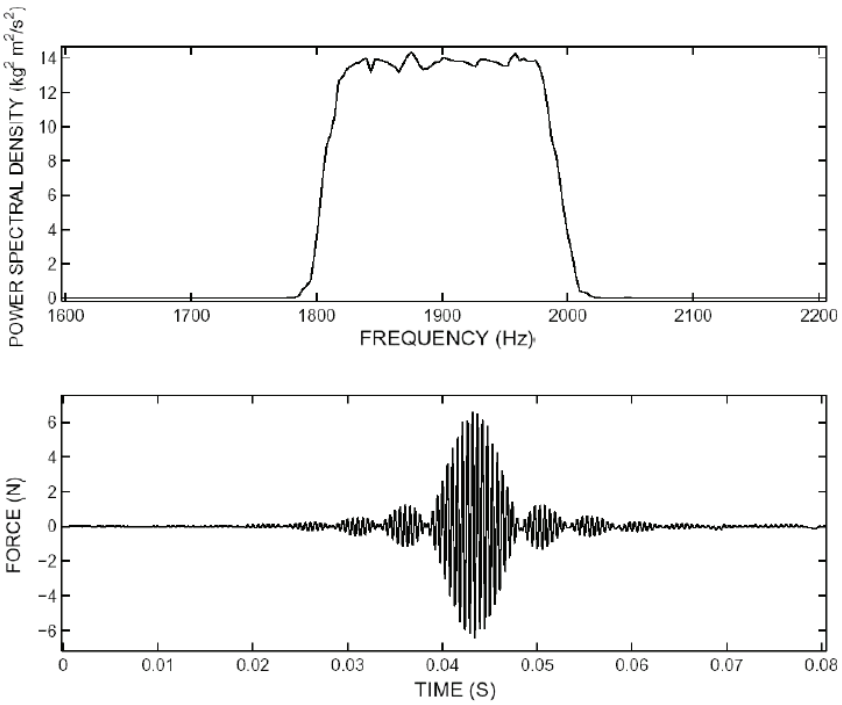
POWER SPECTRAL DENSITY (kg² m²/s²)
14
12
10
8
6
4
2
0
1600
1700
1800
1900
2000
2100
2200
FREQUENCY (Hz)
FORCE (N)
6
4
2
0
−2
−4
−6
0
0.01
0.02
0.03
0.04
0.05
0.06
0.07
0.08
TIME (S)

FIGURE 5

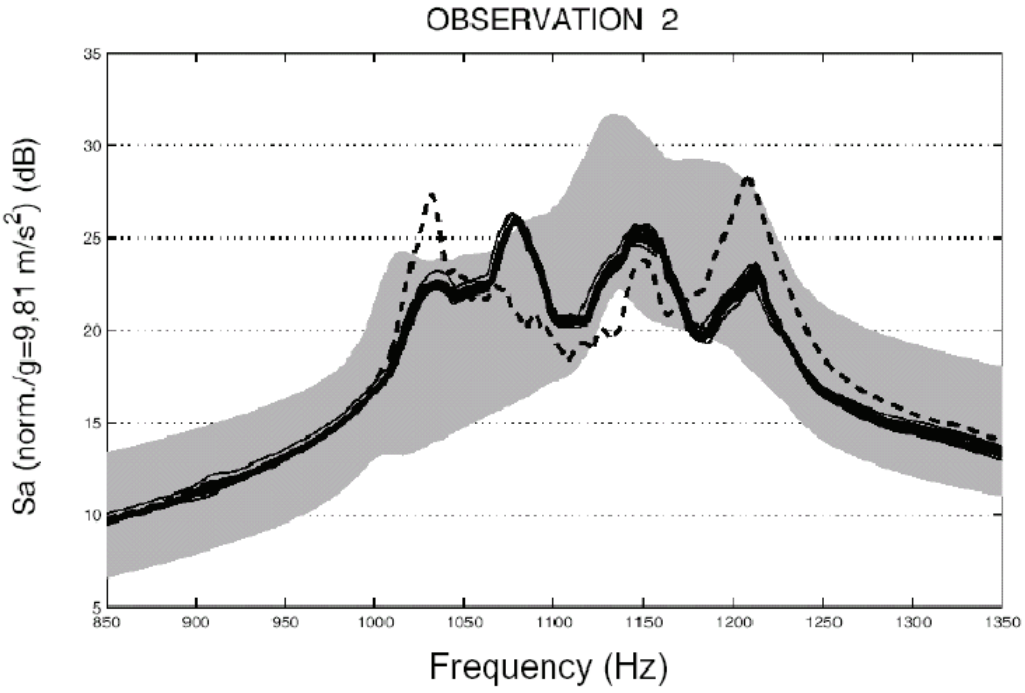
OBSERVATION 2
Sa (norm./g=9,81 m/s²) (dB)
35
30
25
20
15
10
5
850
900
950
1000
1050
1100
1150
1200
1250
1300
1350
Frequency (Hz)

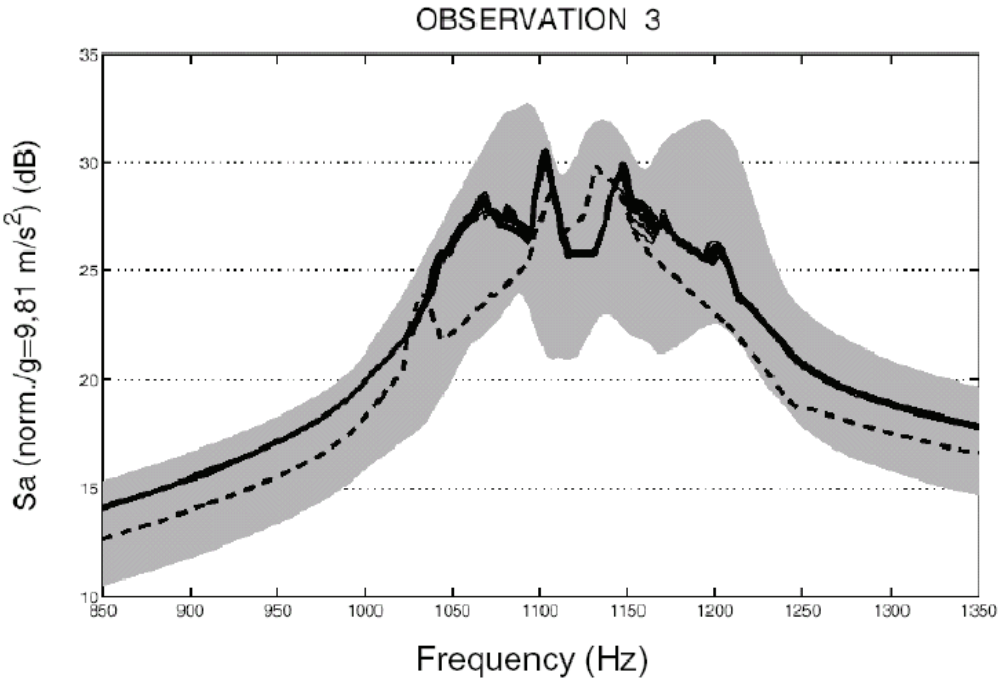
OBSERVATION 3
Sa (norm./g=9,81 m/s²) (dB)
35
30
25
20
15
10
850
900
950
1000
1050
1100
1150
1200
1250
1300
1350
Frequency (Hz)

FIGURE 6

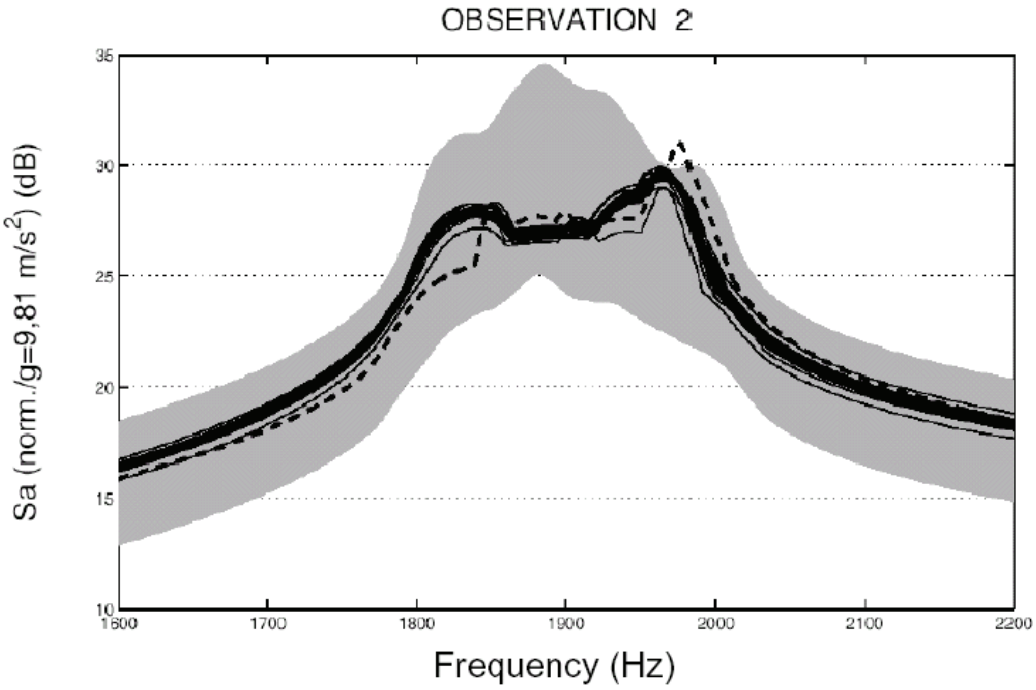
OBSERVATION 2
Sa (norm./g=9,81 m/s^2) (dB)
35
30
25
20
15
10
1600
1700
1800
1900
2000
2100
2200
Frequency (Hz)

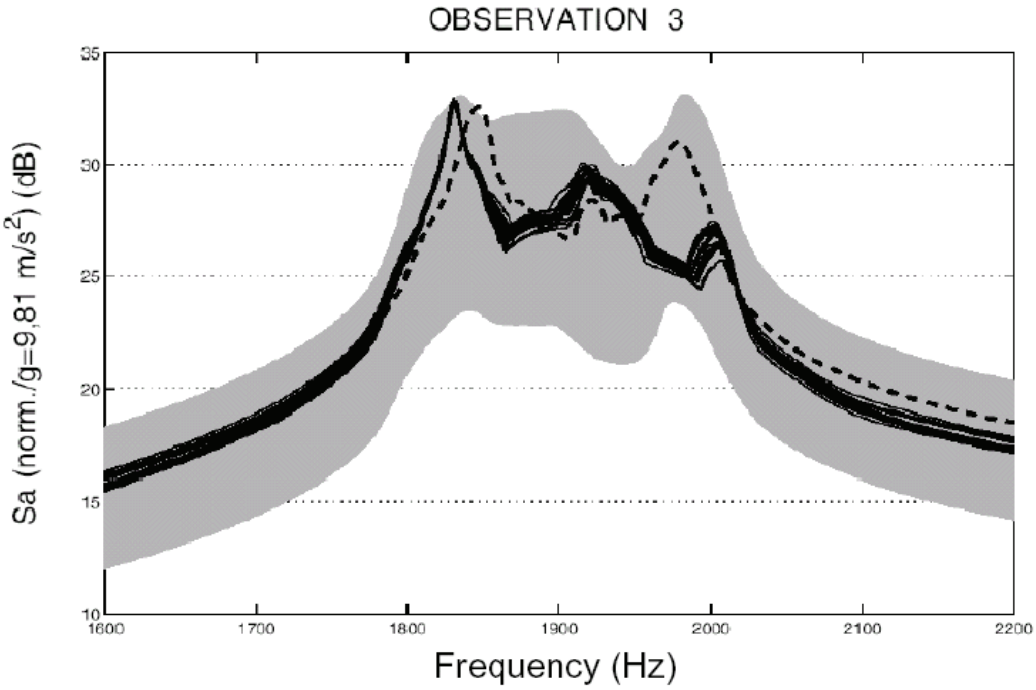
OBSERVATION 3
Sa (norm./g=9,81 m/s^2) (dB)
35
30
25
20
15
10
1600
1700
1800
1900
2000
2100
2200
Frequency (Hz)

FIGURE LEGENDS

Figure 1. Shock response spectrum method

Figure 2. Geometry of the experimental configuration

Figure 3. Excitation load in [1000-1200] Hz

Figure 4. Excitation load in [1800-2000] Hz

Figure 5. SRS at the observation points 2 and 3 for an impulsive load in the band [1000-1200] Hz with $\delta_M^{CJ} = 0$, $\delta_D^{CJ} = 0.8$, $\delta_K^{CJ} = 0.7$, $\delta_M^{plates} = 0$, $\delta_D^{plates} = 0$ and $\delta_K^{plates} = 0.1$.

Figure 6. SRS at the observation points 2 and 3 for an impulsive load in band [1800-2000] Hz with $\delta_M^{CJ} = 0$, $\delta_D^{CJ} = 0.8$, $\delta_K^{CJ} = 0.7$, $\delta_M^{plates} = 0$, $\delta_D^{plates} = 0$ and $\delta_K^{plates} = 0.1$.